US012123932B2

(12) **United States Patent**
Tamada et al.

(10) **Patent No.: US 12,123,932 B2**
(45) **Date of Patent: Oct. 22, 2024**

(54) **SYSTEM AND METHOD FOR QUANTITATIVE MAPPING WITH MAGNETIC RESONANCE IMAGING**

(71) Applicant: **Wisconsin Alumni Research Foundation**, Madison, WI (US)

(72) Inventors: **Daiki Tamada**, Madison, WI (US); **Scott B. Reeder**, Middleton, WI (US)

(73) Assignee: **WISCONSIN ALUMNI RESEARCH FOUNDATION**, Madison, WI (US)

(*) Notice: Subject to any disclaimer, the term of this patent is extended or adjusted under 35 U.S.C. 154(b) by 854 days.

(21) Appl. No.: **17/221,280**

(22) Filed: **Apr. 2, 2021**

(65) **Prior Publication Data**

US 2022/0326327 A1 Oct. 13, 2022

(51) **Int. Cl.**

G01R 33/48	(2006.01)
G01R 33/36	(2006.01)
G01R 33/44	(2006.01)
G01R 33/561	(2006.01)
G01R 33/565	(2006.01)

(52) **U.S. Cl.**

CPC ***G01R 33/4828*** (2013.01); ***G01R 33/3621*** (2013.01); ***G01R 33/445*** (2013.01); ***G01R 33/5615*** (2013.01); ***G01R 33/56518*** (2013.01); ***G01R 33/56554*** (2013.01)

(58) **Field of Classification Search**

CPC G01R 33/4828; G01R 33/3621; G01R 33/445; G01R 33/5615; G01R 33/56518; G01R 33/56554

See application file for complete search history.

(56) **References Cited**

U.S. PATENT DOCUMENTS

10,845,466	B2	11/2020	Reeder et al.	
2007/0152666	A1*	7/2007	Thesen	G01N 24/08 324/306
2015/0160321	A1*	6/2015	Patil	G01R 33/56563 324/309
2016/0084928	A1*	3/2016	Ouyang	G01R 33/5605 324/309
2016/0313423	A1*	10/2016	Eggers	G01R 33/56563
2018/0088197	A1*	3/2018	Suh	G01R 33/5608
2018/0136300	A1*	5/2018	De Rochefort	G01R 33/54

(Continued)

OTHER PUBLICATIONS

Brittain JH, Hu BS, Wright GA, Meyer CH, Macovski A, Nishimura DG. Coronary angiography with magnetization-prepared T2 contrast. Magnetic resonance in medicine 1995;33(5):689-696.

(Continued)

Primary Examiner — Sean A Frith

(74) *Attorney, Agent, or Firm* — Quarles & Brady, LLP

(57) **ABSTRACT**

A system and method are provided for producing at least one of an image or a map of a subject includes controlling a magnetic resonance imaging (MRI) system to perform a pulse sequence that includes a phase increment of an RF pulse selected to induce a phase difference between two echoes at different echo times (TE). The method also includes controlling the MRI system to acquire MR data corresponding to at least the two echoes at different TEs, deriving a static magnetic field (B0) map of the MRI system using the MR data corresponding to the two echoes, and using the B0 map and MR data from at least one of the two echoes, generate a map of T2 of the subject.

20 Claims, 8 Drawing Sheets

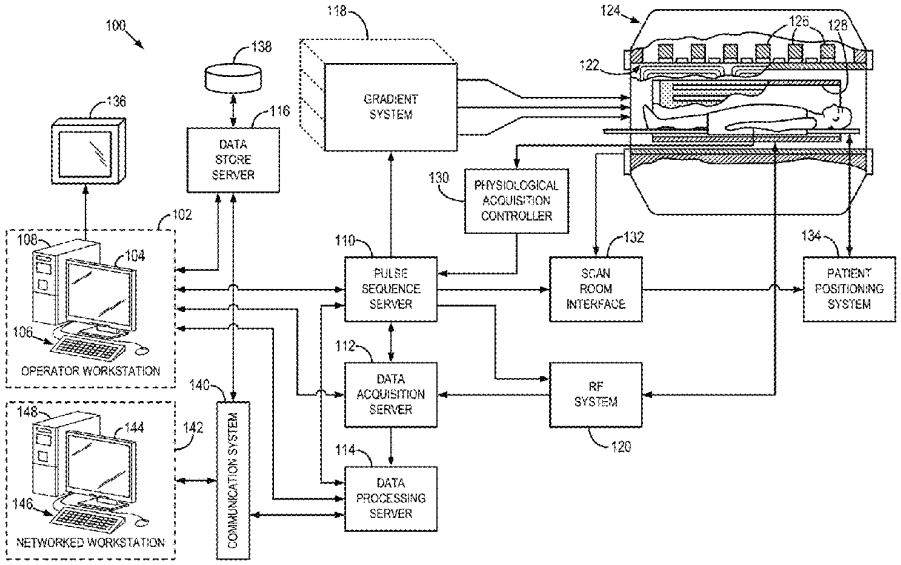

(56) **References Cited**

U.S. PATENT DOCUMENTS

2018/0292488	A1*	10/2018	Moeller	G01R 33/5616
2019/0212407	A1*	7/2019	Köhler	G01R 33/56518
2019/0242961	A1*	8/2019	Meineke	G01R 33/443
2020/0249299	A1*	8/2020	Botnar	G06T 7/0012
2020/0278406	A1*	9/2020	Sharma	G01R 33/4828
2020/0348382	A1*	11/2020	Keupp	A61B 5/055

OTHER PUBLICATIONS

Crawley AP, Wood ML, Henkelman RM. Elimination of transverse coherences in FLASH MRI. Magnetic resonance in medicine 1988;8(3):248-260.

Deoni SC, Rutt BK, Peters TM. Rapid combined T1 and T2 mapping using gradient recalled acquisition in the steady state. Magnetic Resonance in Medicine: An Official Journal of the International Society for Magnetic Resonance in Medicine 2003;49(3):515-526.

Dregely I, Margolis DA, Sung K, Zhou Z, Rangwala N, Raman SS, Wu HH. Rapid quantitative T2 mapping of the prostate using three-dimensional dual echo steady state MRI at 3T. Magnetic Resonance in Medicine 2016;76(6):1720-1729.

Hennig J. Echoes—how to generate, recognize, use or avoid them in MR-imaging sequences. Part II: Echoes in imaging sequences. Concepts in Magnetic Resonance 1991;3(4):179-192.

Huang TY, Liu YJ, Stemmer A, Poncelet BP. T2 measurement of the human myocardium using a T2-prepared transient-state TrueFISP sequence. Magnetic Resonance in Medicine: An Official Journal of the International Society for Magnetic Resonance in Medicine 2007;57(5):960-966.

Reeder SB, Wen Z, Yu H, Pineda AR, Gold GE, Markl M, Pelc NJ. Multicoil Dixon chemical species separation with an iterative least-squares estimation method. Magnetic Resonance in Medicine: An Official Journal of the International Society for Magnetic Resonance in Medicine 2004;51(1):35-45.

Sobol WT, Gauntt DM. On the stationary states in gradient echo imaging. Journal of Magnetic Resonance Imaging 1996;6(2):384-398.

Sveinsson B, Chaudhari A, Gold G, Hargreaves B. A simple analytic method for estimating T2 in the knee from DESS. Magnetic resonance imaging 2017;38:63-70.

Wang X, Hernando D, Reeder SB. Phase-based T2 mapping with gradient echo imaging. Magnetic Resonance in Medicine 2019.

Yarnykh VL. Optimal radiofrequency and gradient spoiling for improved accuracy of T1 and B1 measurements using fast steady-state techniques. Magnetic Resonance in Medicine: An Official Journal of the International Society for Magnetic Resonance in Medicine 2010;63(6):1610-1626.

Yu H, Shimakawa A, McKenzie CA, Brodskky E, Brittain JH, Reeder SB, "Multiecho water-fat separation and simultaneous R2* estimation with multifrequency fat spectrum modeling", Magnetic Resonance in Medicine: Offical Journal of the Society of Magnetic Resonance in Medicine/Society of Magnetic Resonance in Medicine 2008; 60(5):1122-1134.

Zur Y, Wood M, Neuringer L. Spoiling of transverse magnetization in steady-state sequences. Magnetic resonance in medicine 1991;21(2):251-263.

* cited by examiner

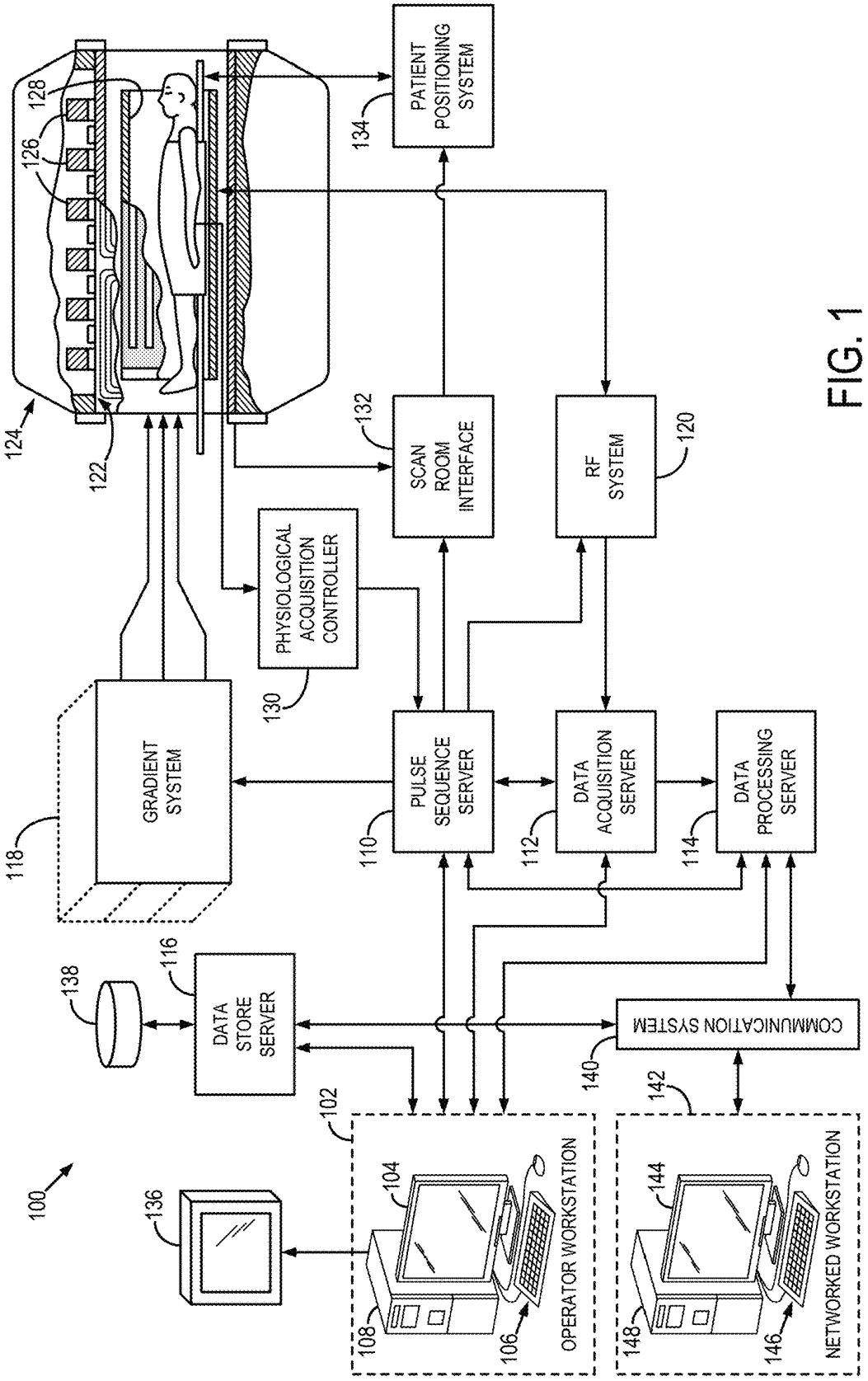
100
102
104
106
108
110
112
114
116
118
120
122
124
126
128
130
132
134
136
138
140
142
144
146
148
PATIENT POSITIONING SYSTEM
SCAN ROOM INTERFACE
RF SYSTEM
PHYSIOLOGICAL ACQUISITION CONTROLLER
GRADIENT SYSTEM
PULSE SEQUENCE SERVER
DATA ACQUISITION SERVER
DATA PROCESSING SERVER
DATA STORE SERVER
COMMUNICATION SYSTEM
OPERATOR WORKSTATION
NETWORKED WORKSTATION

FIG. 1

FIG. 2

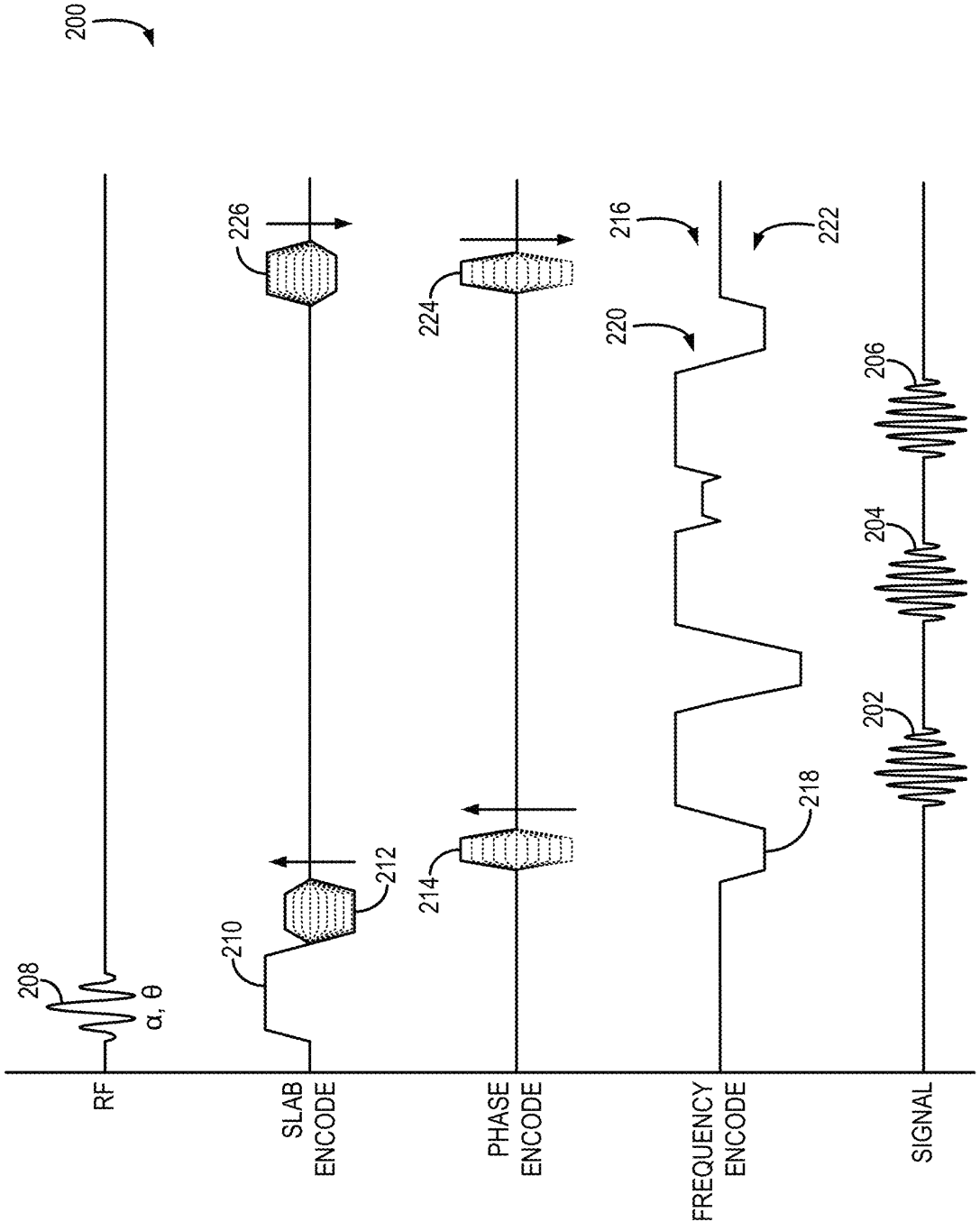
200
RF
SLAB ENCODE
PHASE ENCODE
FREQUENCY ENCODE
SIGNAL
208
α, θ
210
212
214
224
226
216
218
220
222
202
204
206

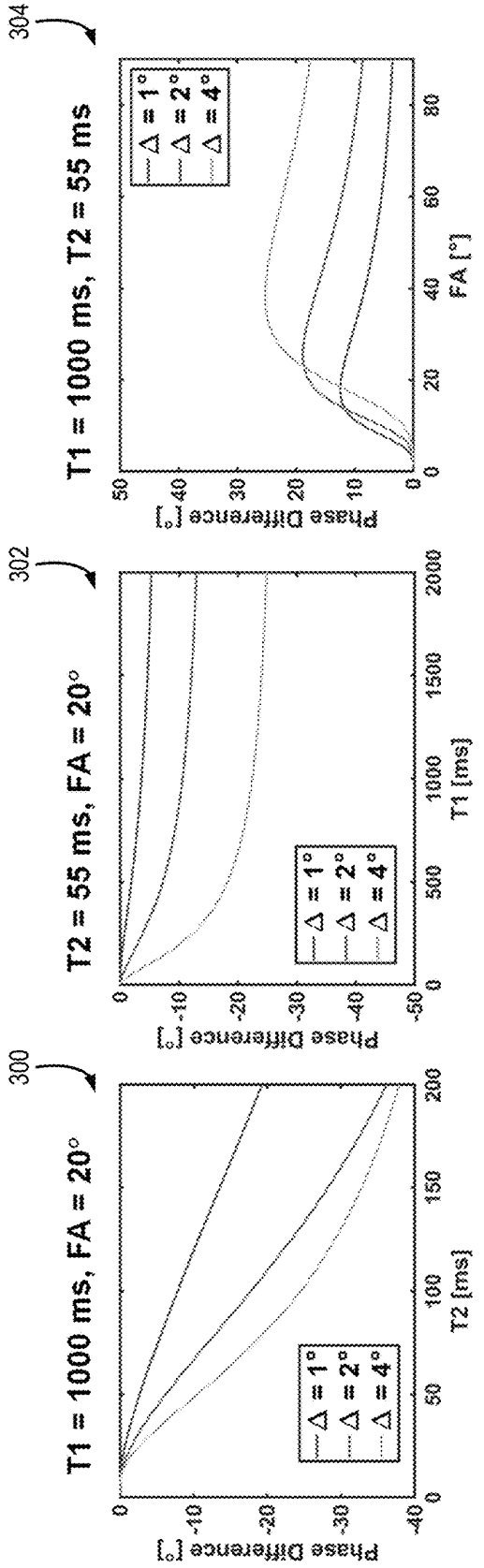
304
T1 = 1000 ms, T2 = 55 ms
Δ = 1°
Δ = 2°
Δ = 4°
Phase Difference [°]
FA [°]
302
T2 = 55 ms, FA = 20°
T1 [ms]
300
T1 = 1000 ms, FA = 20°
T2 [ms]

FIG. 3

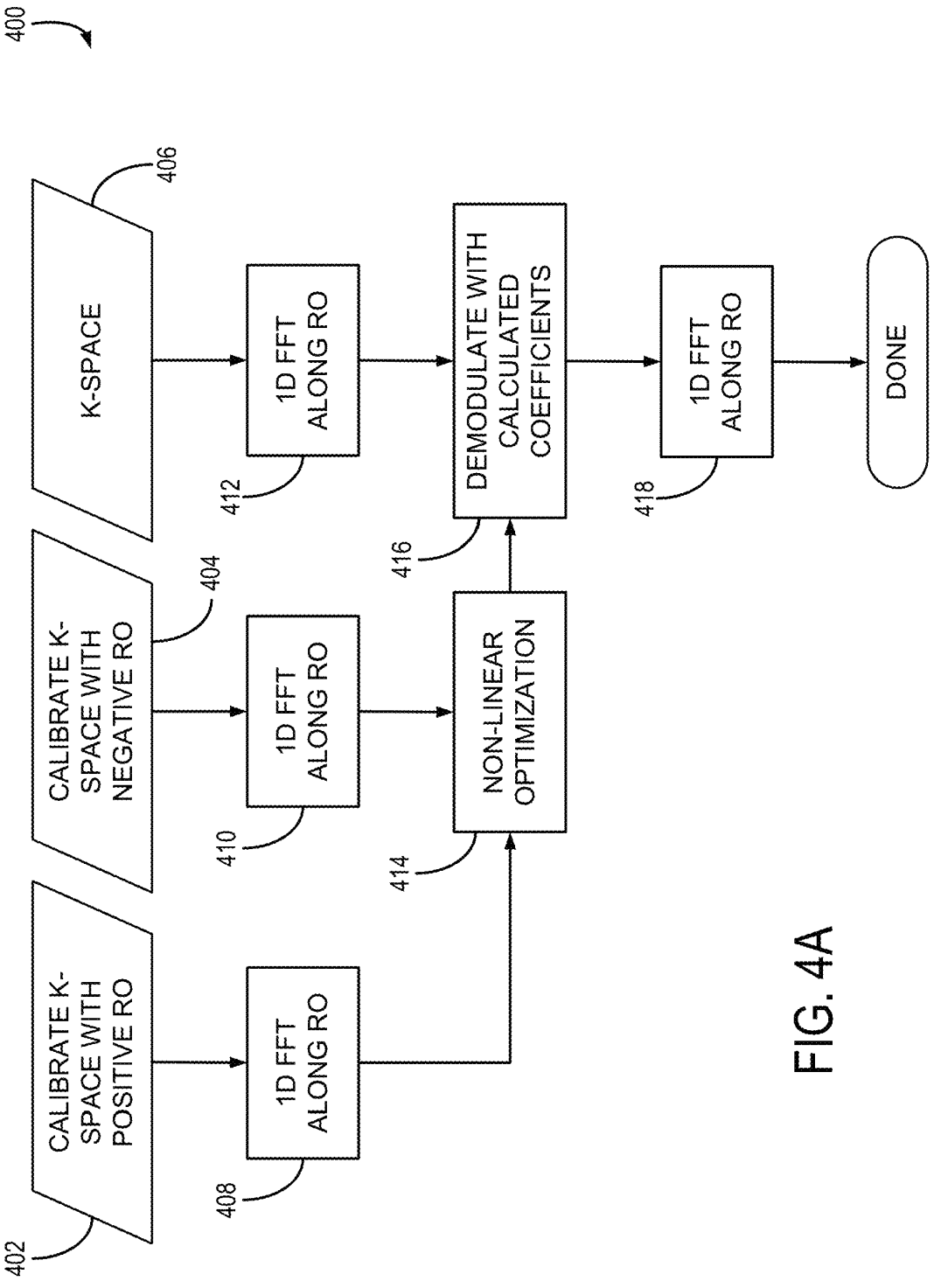
400
CALIBRATE K-SPACE WITH POSITIVE RO
402
CALIBRATE K-SPACE WITH NEGATIVE RO
404
K-SPACE
406
1D FFT ALONG RO
408
1D FFT ALONG RO
410
1D FFT ALONG RO
412
NON-LINEAR OPTIMIZATION
414
DEMODULATE WITH CALCULATED COEFFICIENTS
416
1D FFT ALONG RO
418
DONE

FIG. 4A

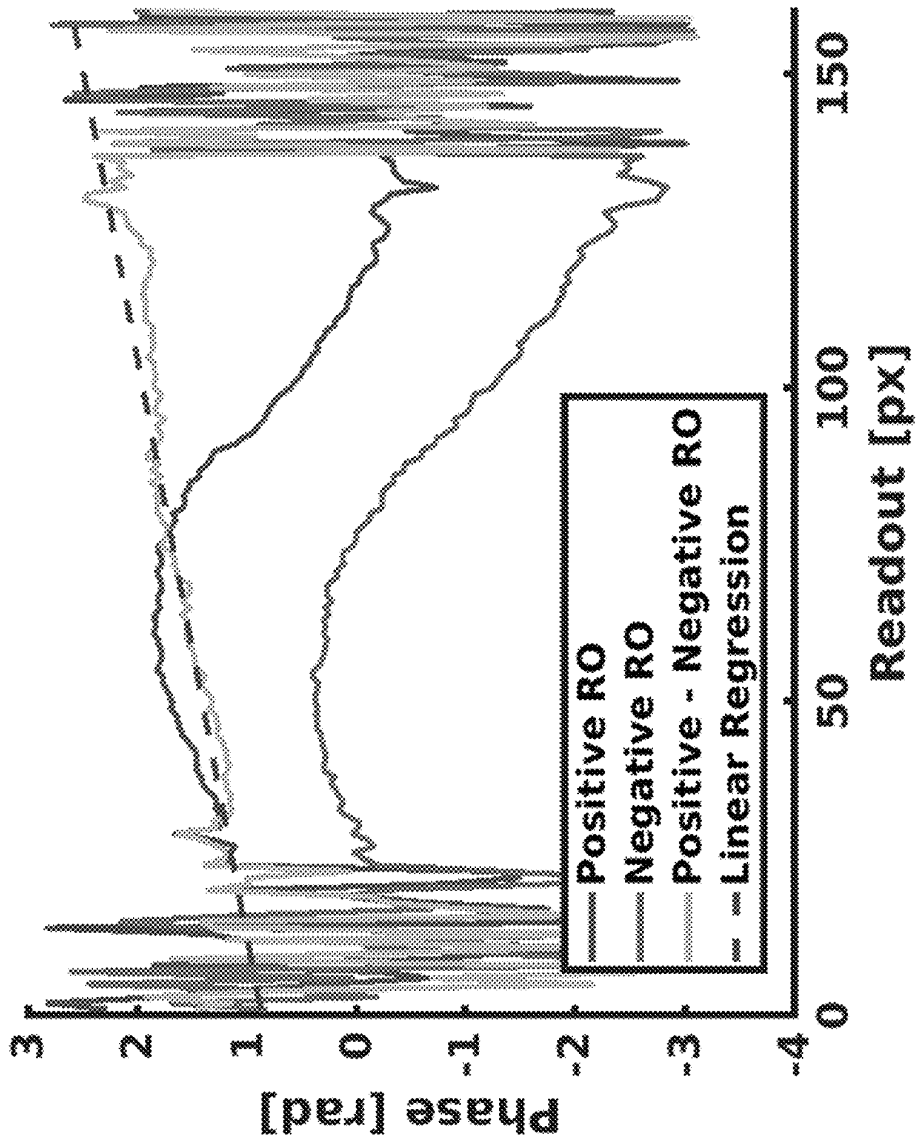
Phase [rad]
3
2
1
0
-1
-2
-3
-4
0
50
100
150
Readout [px]
Positive RO
Negative RO
Positive - Negative RO
Linear Regression

FIG. 4B

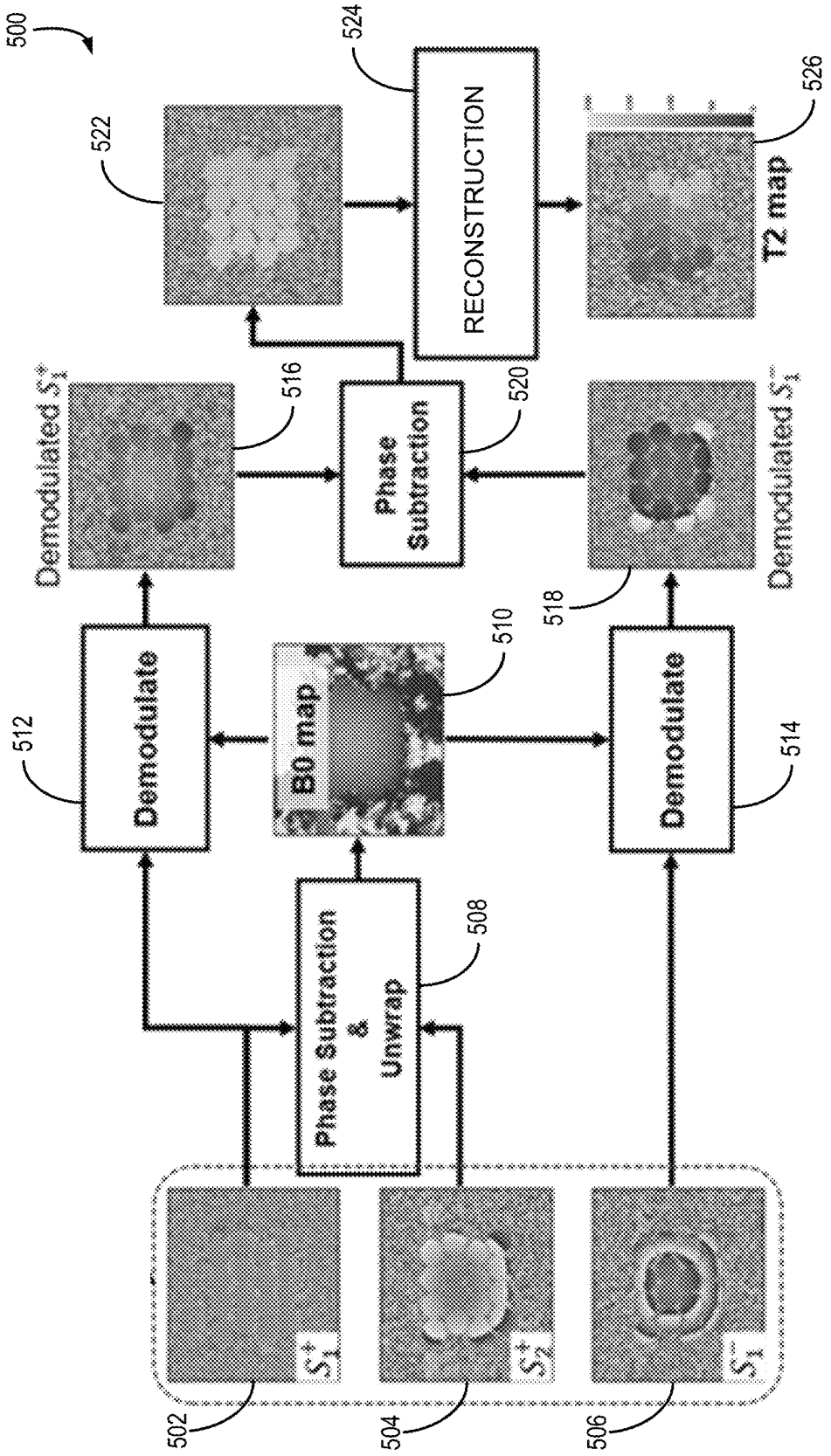
500
524
RECONSTRUCTION
522
526
T2 map
Demodulated S_1^+
516
Phase Subtraction
520
Demodulated S_1^-
518
510
512
Demodulate
B0 map
Demodulate
514
508
Phase Subtraction & Unwrap
S_1^+
S_2^+
S_1^-
502
504
506

FIG. 5

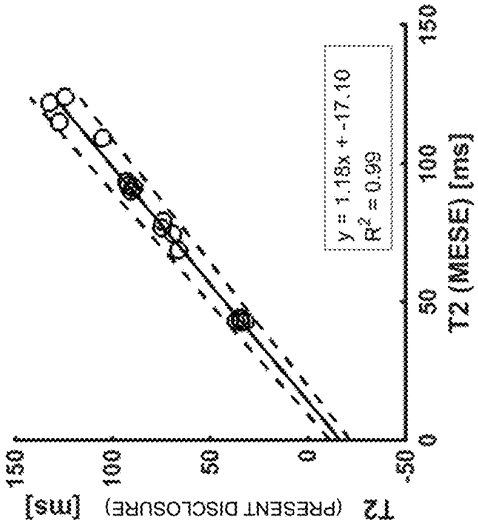

FIG. 6C

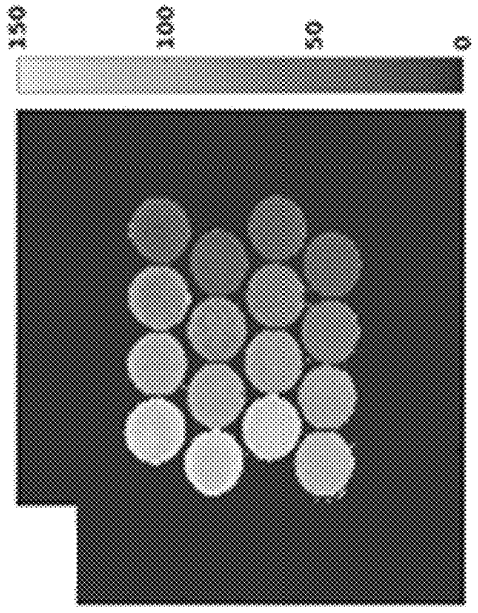

FIG. 6B

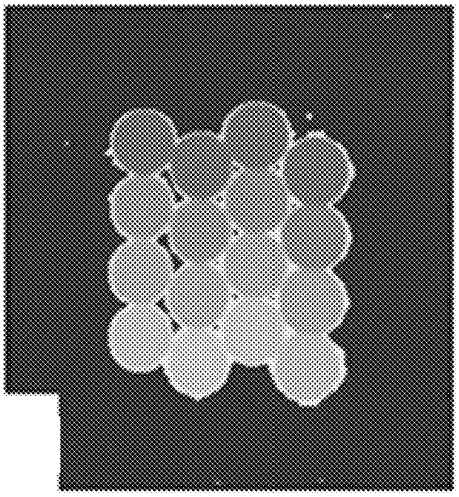

FIG. 6A

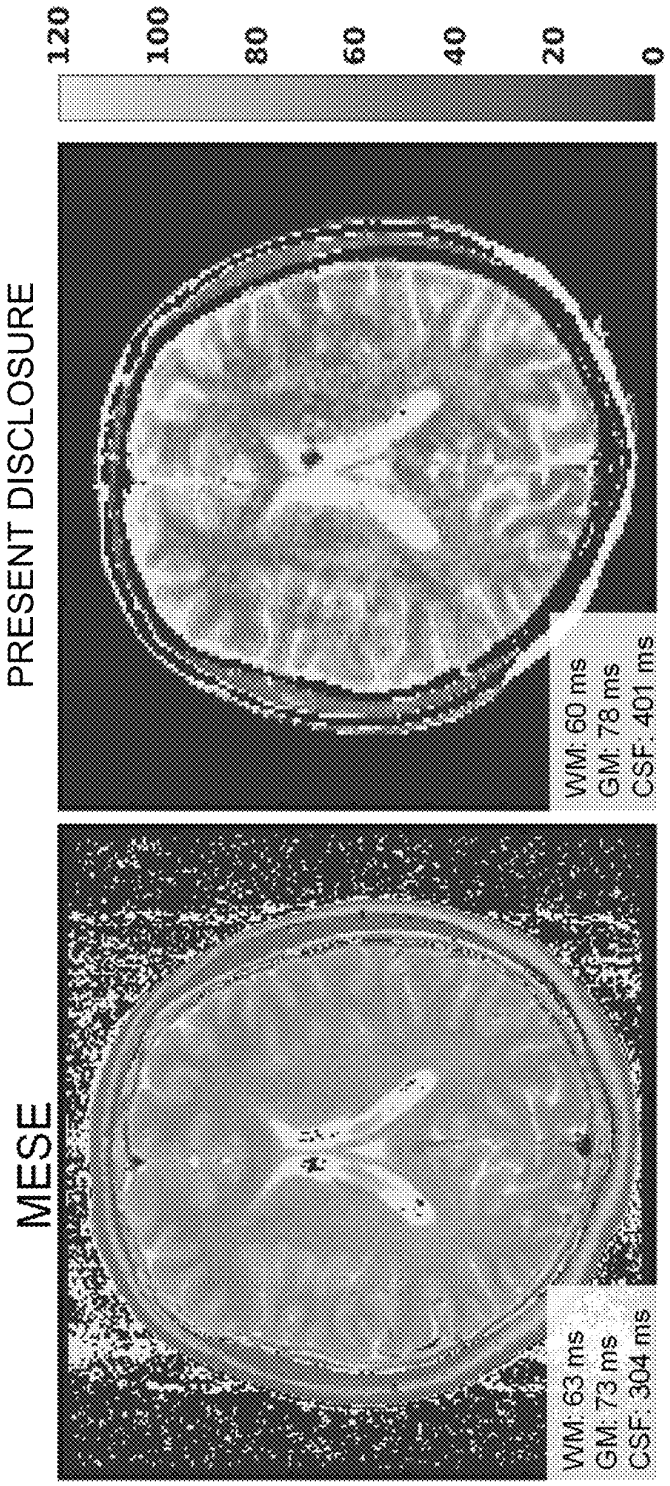
120
100
80
60
40
20
0
PRESENT DISCLOSURE
WM: 60 ms
GM: 78 ms
CSF: 401 ms
MESE
WM: 63 ms
GM: 73 ms
CSF: 304 ms

FIG. 7

SYSTEM AND METHOD FOR QUANTITATIVE MAPPING WITH MAGNETIC RESONANCE IMAGING

STATEMENT REGARDING FEDERALLY SPONSORED RESEARCH

N/A

BACKGROUND

The field of the disclosure is systems and methods for magnetic resonance imaging (MRI). More particularly, the invention relates to systems and methods for magnetic resonance imaging to produce quantitative maps.

When a substance, such as human tissue, is subjected to a uniform magnetic field (polarizing field B_0), the individual magnetic moments of the nuclei in the tissue attempt to align with this polarizing field, but precess about it in random order at their characteristic Larmor frequency. If the substance, or tissue, is subjected to a magnetic field (excitation field B_1) that is in the x-y plane and that is near the Larmor frequency, the net aligned moment, M_z, may be rotated, or "tipped", into the x-y plane to produce a net transverse magnetic moment, M_{xy}. A signal is emitted by the excited nuclei or "spins", after the excitation signal B_1 is terminated, and this signal may be received and processed to form an image.

When utilizing these "MR" signals to produce images, magnetic field gradients (G_x, G_y, and G_z) are employed. Typically, the region to be imaged is scanned by a sequence of measurement cycles in which these gradients vary according to the particular localization method being used. The resulting set of received MR signals are digitized and processed to reconstruct the image using one of many well-known reconstruction techniques.

To do so, the signals are often weighted in different ways to give preference to or consider different sub-signals or so-called contrast mechanisms. Two basic "contrast mechanisms" commonly utilized in MR imaging are the spin-lattice (or longitudinal or T1) relaxation time or spin-spin (or transverse or T2) relaxation time. The T1 and T2 contrast mechanism are the two most important relaxation mechanisms commonly exploited to provide soft tissue contrast in clinical MRI examinations. Both T1- and T2-weighted (T1w, T2w) acquisitions play a ubiquitous role in almost every clinical MRI exam and are important for a variety of applications including lesion detection, characterization, treatment monitoring, and many other applications. However, there are a variety of other mechanisms for eliciting contrast in MRI, including R2*. Specifically, T2* is a quantity related to T2, but including dephasing effects. That is, T2* is a quantity related to spin-spin relaxation and, in addition, relating magnetic field inhomogeneities and susceptibility effects.

These contrast mechanisms can be manipulated by selecting particular imaging parameters utilized while performing a pulse sequence to acquire MR data, so that the images reconstructed form the MR data reflect a particular weighting toward the preferred contrast mechanism that best illustrate the underlying anatomy or pathology that is the focus of the clinical analysis. Since the fundamentals of the pulse sequence and the imaging parameters dictate the contrast weighting, a variety of different pulse sequences and variations on pulse sequences have been developed.

Beyond controlling these contrast mechanisms for purposes of creating anatomical images, which convey qualitative information about the illustrated anatomical structures via the relative contrast in the images, there have been concerted efforts to elicit quantitative information from MR data. For example, instead of qualitative images, some have created quantitative maps using MR data. For example, quantitative T2 mapping has gained attention as a promising approach for the diagnosis and evaluation of various diseases. The so-called Carr-Purcell-Meiboom-Gill sequence is the most commonly used approach for quantifying T2. Other approaches to T2 mapping include the use of T2-prep (Brittain J H, Hu B S, Wright G A, Meyer C H, Macovski A, Nishimura D G. Coronary angiography with magnetization-prepared T2 contrast. Magnetic resonance in medicine 1995; 33(5):689-696.) and balanced steady-state free precession (Huang T Y, Liu Y J, Stemmer A, Poncelet B P. T2 measurement of the human myocardium using a T2-prepared transient-state TrueFISP sequence. Magnetic Resonance in Medicine: An Official Journal of the International Society for Magnetic Resonance in Medicine 2007; 57(5): 960-966.).

Some studies have explored simultaneous T1, T2 and ADC mapping with methods including diffusion-weighted dual-echo steady state (DESS). However, these techniques face substantial limitations. For the DESS method, the signal from steady-state sequence is complicated to model, especially with diffusion encoding, which may result in inaccuracy and large variance in diffusion measurements. Recently, a phase-based T2 mapping method that encodes T2 information into phase of RF phase modulated gradient echo signal has been proposed and demonstrated (Wang X, Hernando D, Reeder S B. Phase-based T2 mapping with gradient echo imaging. Magnetic Resonance in Medicine 2019 and U.S. Pat. No. 10,845,446, both of which are incorporated herein by reference).

Unfortunately, despite the ability to perform T2 mapping using these techniques, each techniques includes appreciable drawbacks. For example, these techniques require extended acquisition times, which increase the risk of motion artifacts or other challenges in data acquisition.

Thus, there is a continuing need for new MRI data acquisition, data processing, and/or image reconstruction techniques, for generating quantitative maps from MR data.

SUMMARY

The present disclosure overcomes the aforementioned drawbacks by providing systems and methods for performing quantitative mapping using a phase-based approach. For example, RF phase modulation can be used to elicit MR data suitable for quantitative mapping. The systems and methods provided herein are more efficient and less prone to artifacts or errors, such as caused by misregistration of acquisitions.

In accordance with one aspect of the disclosure, a magnetic resonance imaging (MRI) system is provided that includes a magnet system configured to generate a polarizing magnetic field about at least a portion of a subject arranged in the MRI system and a plurality of gradient coils configured to apply magnetic gradients to the polarizing magnetic field. The MRI system further includes a radio frequency (RF) system configured to apply an excitation field to the subject and acquire MR image data from the subject and a computer system. The computer system is programmed to control the plurality of gradient coils and the RF system to perform a gradient echo pulse sequence that includes a phase increment of an RF pulse of the gradient echo pulse sequence selected to induce a phase difference between two echoes selected to be similar, other than echo

time (TE). The computer system is also configured to control the RF system to acquire MR data corresponding to at least the two echoes selected to be similar, other than TE and derive a B_0 map using the MR data corresponding to the two echoes selected to be similar, other than TE. The computer system is further programmed to use the B_0 map and MR data from at least one of the two echoes selected to be similar, other than TE, generate a map of T2 of the subject.

In accordance with another aspect of the disclosure, a method is provided for producing at least one of an image or a map of a subject includes controlling a magnetic resonance imaging (MRI) system to perform a pulse sequence that includes a phase increment of an RF pulse selected to induce a phase difference between two echoes at different echo times (TE). The method also includes controlling the MRI system to acquire MR data corresponding to at least the two echoes at different TEs, deriving a static magnetic field (B0) map of the MRI system using the MR data corresponding to the two echoes, and using the B0 map and MR data from at least one of the two echoes, generate a map of T2 of the subject.

The foregoing and other aspects and advantages of the invention will appear from the following description. In the description, reference is made to the accompanying drawings, which form a part hereof, and in which there is shown by way of illustration a preferred embodiment of the invention. Such embodiment does not necessarily represent the full scope of the invention, however, and reference is made therefore to the claims and herein for interpreting the scope of the invention.

BRIEF DESCRIPTION OF THE DRAWINGS

FIG. **1** is a block diagram of an exemplary magnetic resonance imaging (MRI) system configured in accordance with the present disclosure.

FIG. **2** is a graphic representation of an exemplary pulse sequence for directing the MRI system of FIG. **1** in accordance with the present disclosure.

FIG. **3** is a set of correlated graphs showing phase difference plotted against T2, and T1, and FA.

FIG. **4**A is a flow chart setting forth some non-limiting examples steps of a process for correcting for eddy current induced phase.

FIG. **4**B is a graph showing coefficients of signal components of each echo can be determined by fitting the phase difference between signals with positive and negative readout since only the eddy current-induced phase depends on the polarity of the gradient.

FIG. **5** is a flow chart setting forth some non-limiting examples steps of a process for a reconstruction strategy in accordance with one aspect of the present disclosure.

FIG. **6**A is an image of a phantom acquired using a multi-echo spin echo (MESE) acquisition.

FIG. **6**B is an image of a phantom acquired using a process in accordance with the present disclosure.

FIG. **6**C is a graph showing T2 mapped from the data corresponding to FIG. **6**A against data corresponding to FIG. **6**B.

FIG. **7** is a set of images showing T2 maps for a volunteer brain measured using a MESE pulse sequence and a pulse sequence in accordance with the present disclosure.

DETAILED DESCRIPTION

When seeking to provide quantitative maps using MR data, some have used the magnitude signal from dual echo steady-state (DESS), and triple echo steady-state pulse sequences for rapid T2 mapping. Furthermore, a phase-based T2 mapping method that encodes T2 information into phase of RF phase modulated gradient echo signal has been proposed and demonstrated (Wang X, Hernando D, Reeder S B. Phase-based T2 mapping with gradient echo imaging. Magnetic Resonance in Medicine 2019 and U.S. Pat. No. 10,845,446, both of which are incorporated herein by reference). Despite rapid and reliable T2 mapping using the phase-based approach, two-pass imaging is required to subtract background phase. This doubles the acquisition time and can result in misregistration between the two separate acquisitions. Thus, as will be described, the present disclosures provides systems and methods for performing T2 mapping using a phase-based approach, whereby RF phase modulation is used, for example, with a pulse sequence such as the DESS or triple echo pulse sequences.

Referring now to FIG. **1**, a magnetic resonance imaging (MRI) system **100** is provided that may be configured, programmed, or otherwise utilized in accordance with the present disclosure. The MRI system **100** includes an operator workstation **102**, which will typically include a display **104**, one or more input devices **106** (such as a keyboard and mouse or the like), and a processor **108**. The processor **108** may include a commercially available programmable machine running a commercially available operating system. The operator workstation **102** provides the operator interface that enables scan prescriptions to be entered into the MRI system **100**. In general, the operator workstation **102** may be coupled to multiple servers, including a pulse sequence server **110**; a data acquisition server **112**; a data processing server **114**; and a data store server **116**. The operator workstation **102** and each server **110**, **112**, **114**, and **116** are connected to communicate with each other. For example, the servers **110**, **112**, **114**, and **116** may be connected via a communication system **140**, which may include any suitable network connection, whether wired, wireless, or a combination of both. As an example, the communication system **140** may include both proprietary or dedicated networks, as well as open networks, such as the internet.

The pulse sequence server **110** functions in response to instructions downloaded from the operator workstation **102** to operate a gradient system **118** and a radiofrequency (RF) system **120**. Gradient waveforms to perform the prescribed scan are produced and applied to the gradient system **118**, which excites gradient coils in an assembly **122** to produce the magnetic field gradients G_x, G_y, G_z used for position encoding magnetic resonance signals. The gradient coil assembly **122** forms part of a magnet assembly **124** that includes a polarizing magnet **126** and a whole-body RF coil **128**.

RF waveforms are applied by the RF system **120** to the RF coil **128**, or a separate local coil (not shown in FIG. **1**), in order to perform the prescribed magnetic resonance pulse sequence. Responsive magnetic resonance signals detected by the RF coil **128**, or a separate local coil, are received by the RF system **120**, where they are amplified, demodulated, filtered, and digitized under direction of commands produced by the pulse sequence server **110**. The RF system **120** includes an RF transmitter for producing a wide variety of RF pulses used in MRI pulse sequences. The RF transmitter is responsive to the scan prescription and direction from the pulse sequence server **110** to produce RF pulses of the desired frequency, phase, and pulse amplitude waveform. The generated RF pulses may be applied to the whole-body RF coil **128** or to one or more local coils or coil arrays.

The RF system **120** also includes one or more RF receiver channels. Each RF receiver channel includes an RF preamplifier that amplifies the magnetic resonance signal received by the coil **128** to which it is connected, and a detector that detects and digitizes the I and Q quadrature components of the received magnetic resonance signal. The magnitude of the received magnetic resonance signal may, therefore, be determined at any sampled point by the square root of the sum of the squares of the I and Q components:

$$M=\sqrt{I^2+Q^2} \quad \text{Eqn. 1;}$$

and the phase of the received magnetic resonance signal may also be determined according to the following relationship:

$$\varphi = \tan^{-1}\left(\frac{Q}{I}\right). \quad \text{Eqn. 2}$$

The pulse sequence server **110** also optionally receives patient data from a physiological acquisition controller **130**. By way of example, the physiological acquisition controller **130** may receive signals from a number of different sensors connected to the patient, such as electrocardiograph (ECG) signals from electrodes, or respiratory signals from a respiratory bellows or other respiratory monitoring device. Such signals are typically used by the pulse sequence server **110** to synchronize, or "gate," the performance of the scan with the subject's heart beat or respiration.

The pulse sequence server **110** also connects to a scan room interface circuit **132** that receives signals from various sensors associated with the condition of the patient and the magnet system. It is also through the scan room interface circuit **132** that a patient positioning system **134** receives commands to move the patient to desired positions during the scan.

The digitized magnetic resonance signal samples produced by the RF system **120** are received by the data acquisition server **112**. The data acquisition server **112** operates in response to instructions downloaded from the operator workstation **102** to receive the real-time magnetic resonance data and provide buffer storage, such that no data are lost by data overrun. In some scans, the data acquisition server **112** does little more than pass the acquired magnetic resonance data to the data processor server **114**. However, in scans that require information derived from acquired magnetic resonance data to control the further performance of the scan, the data acquisition server **112** is programmed to produce such information and convey it to the pulse sequence server **110**. For example, during prescans, magnetic resonance data are acquired and used to calibrate the pulse sequence performed by the pulse sequence server **110**. As another example, navigator signals may be acquired and used to adjust the operating parameters of the RF system **120** or the gradient system **118**, or to control the view order in which k-space is sampled.

The data processing server **114** receives magnetic resonance data from the data acquisition server **112** and processes it in accordance with instructions downloaded from the operator workstation **102**. Such processing may, for example, include one or more of the following: reconstructing two-dimensional or three-dimensional images by performing a Fourier transformation of raw k-space data; performing other image reconstruction techniques, such as iterative or backprojection reconstruction techniques; applying filters to raw k-space data or to reconstructed images; generating functional magnetic resonance images; calculating motion or flow images; and so on.

Images reconstructed by the data processing server **114** are conveyed back to the operator workstation **102**. Images may be output to operator display **112** or a display **136** that is located near the magnet assembly **124** for use by attending clinician. Batch mode images or selected real time images are stored in a host database on disc storage **138**. When such images have been reconstructed and transferred to storage, the data processing server **114** notifies the data store server **116** on the operator workstation **102**. The operator workstation **102** may be used by an operator to archive the images, produce films, or send the images via a network to other facilities.

The MRI system **100** may also include one or more networked workstations **142**. By way of example, a networked workstation **142** may include a display **144**, one or more input devices **146** (such as a keyboard and mouse or the like), and a processor **148**. The networked workstation **142** may be located within the same facility as the operator workstation **102**, or in a different facility, such as a different healthcare institution or clinic. The networked workstation **142** may include a mobile device, including phones or tablets.

The networked workstation **142**, whether within the same facility or in a different facility as the operator workstation **102**, may gain remote access to the data processing server **114** or data store server **116** via the communication system **140**. Accordingly, multiple networked workstations **142** may have access to the data processing server **114** and the data store server **116**. In this manner, magnetic resonance data, reconstructed images, or other data may be exchanged between the data processing server **114** or the data store server **116** and the networked workstations **142**, such that the data or images may be processed remotely by a networked workstation **142**. This data may be exchanged in any suitable format, such as in accordance with the transmission control protocol (TCP), the internet protocol (IP), or other known or suitable protocols.

The above-described MRI system can be used to implement a variety of pulse sequences to effectuate desired imaging studies. As will be described herein, one category of pulse sequence is the gradient echo (GRE) sequence and variations thereof, such as spoiled gradient echo (SGRE) acquisitions. Referring to FIG. **2**, one non-limiting example of a pulse sequence **200** in accordance with the present disclosure is provided. In particular, the pulse sequence **200** of FIG. **2** is a three-echo pulse sequence because it is designed to elicit three echoes **202**, **204**, **206** as the MR signal. As will be explained, the first echo **202** and the second echo **204** are fast imaging with steady-state precession (FISP) or gradient-recalled acquisition in the steady state (GRASS) echoes. The third echo **206** is a time reversed fast imaging with steady state precession (PSIF) echo. In this regard, the pulse sequence **200** can be conceptualized as a variation of a dual echo steady state (DESS) pulse sequence because it is a combination of FISP and PSIF pulse sequences. As will be described, the pulse sequence **200** is a multi-echo T2-enhanced steady-state gradient echo sequence that, in accordance with the present disclosure, allows for a phase-based approach to T2 mapping.

In particular, the pulse sequence **200** includes a radio frequency (RF) pulse **208** that includes a phase increment. For example, the RF excitation pulse **208** may be performed with quadratic phase modulation of θ. A slab-selective gradient **210** with a slab-selective rewinder and slab encoding lobe **212** acts to rephase unwanted phase dispersions

introduced by the slab-selective gradient **210**, such that signal losses resultant from these phase dispersions are mitigated. Following excitation of the nuclear spins in the prescribed imaging slab, a phase encoding gradient **214** is applied to spatially encode the elicited echoes **202**, **204**, **206**, along one direction in the prescribed imaging slab. In addition to phase encoding, a second encoding can be applied transversely, which may be referred to as "depth encoding." As a non-limiting example, if phase encoding is applied in the y-direction, depth encoding may be performed along the z-direction. A series of readout gradients **216** are also applied starting with a dephasing gradient lobe **218** to spatially encode the echoes **202**, **204**, **206** along a second, orthogonal direction in the prescribed imaging slab. More particularly, each acquisition includes of two FISP echoes **202**, **203**, that can be identified as "S_1^+" and "S_2^+". The second echo is followed by PSIF echo, which can be identified as "S_1^-". Thus, "S_1^+" and "S_2^+" can be conceptualized as the same signal sampled at different times, which, as will be described, allows the B_0 field to be derived without further acquisitions.

That is, the two FISP echoes **202**, **204** have different echo times (TEs) and can be used to estimate a B_0 map. The B_0 map can then be used to demodulate B_0 phase components of the S_1^+ echo **202** and S_1^- echo **206**. The RF excitation **208** can be performed with a quadratic increase of transmitting phase to encode T2 information into the phase of the signal/echoes **202**, **204**, **206**. Calibration acquisitions using positive readout gradients **220** and negative gradients **222** without phase-encoding can be incorporated to remove any eddy current-induced phase errors. Calibration acquisitions can be performed using two additional phase encoding lines **224** coupled with a spoiler and slab-encoding gradient rewinder gradient **226**. Though illustrated with three echoes, more echoes could be acquired, including an S_2^- echo, if desired, for example to facilitate fat and water separation. Furthermore, beyond performing water-fat separation, an estimate T2* can be derived from the echoes, such as described, for example, in Yu H, Shimakawa A, McKenzie C A, Brodsky E, Brittain J H, Reeder S B. Multiecho water-fat separation and simultaneous R2* estimation with multifrequency fat spectrum modeling. Magnetic resonance in medicine: official journal of the Society of Magnetic Resonance in Medicine/Society of Magnetic Resonance in Medicine 2008; 60(5):1122-1134, which is incorporated herein by reference.

In order to explain the characteristics and contrast of the steady-state of the above-described, RF phase modulated pulse sequence **200**, one can use an approach such as described in Sobol W T, Gauntt D M. On the stationary states in gradient echo imaging. Journal of Magnetic Resonance Imaging 1996; 6(2):384-398, which is incorporated herein by reference, and which utilizes the configuration theory described in Hennig J. Echoes—how to generate, recognize, use or avoid them in MR-imaging sequences. Part II: Echoes in imaging sequences. Concepts in Magnetic Resonance 1991; 3(4):179-192 and also incorporated herein by reference.

As described, the pulse sequence **200** uses an RF pulse with flip angle (FA) of α, RF phase of ϕ, and repetition time (TR). RF phase modulation can be performed by incrementing the transmit RF phase (ϕ) quadratically. For example, incrementing can be achieved such that $\phi(n)=\phi(n-1)+n\theta$, where θ is the RF phase increment. In this case, the steady-state complex signal (S) after RF excitation can be expressed as:

$$S^+ = \beta(\eta X(-1) + j(\eta^2 - \epsilon(X(-1) - \epsilon))); \quad \text{Eqn. 3}$$

$$S^- = \beta(\eta + j(X(-1) - \epsilon)); \quad \text{Eqn. 4}$$

with

$$\beta = \frac{\left(1 - e^{-\frac{TR}{T1}}\right) M_0 \sin\alpha}{\left(e^{-\frac{TR}{T2}} - \epsilon\right)\left[e^{-\frac{TR}{T2}}\left(\cos\alpha - e^{-\frac{TR}{T1}}\right) + \epsilon\left(1 - e^{-\frac{TR}{T1}}\cos\alpha\right)\right] - \eta^2\left(1 - e^{-\frac{TR}{T1}}\cos\alpha\right)}; \quad \text{Eqn. 5}$$

where M_0 is the proton density, and ϵ and η are real coefficients defined as:

$$\epsilon = \mathrm{Re}\left(\frac{\lambda - \Omega_{22}}{\Omega_{21}}\right); \quad \text{Eqn. 6}$$

$$\eta = \mathrm{Im}\left(\frac{\lambda - \Omega_{22}}{\Omega_{21}}\right); \quad \text{Eqn. 7}$$

with

$$\lambda = \frac{2}{\Omega_{11} + \Omega_{22} + \sqrt{(\Omega_{11} + \Omega_{22})^2 - 4}}; \quad \text{Eqn. 8}$$

where λ, ϵ and η can be determined from the diagonal elements, Ω_{11} and Ω_{22}, of the recursive matrix equation:

$$\begin{bmatrix} \Omega_{11} & \Omega_{21} \\ \Omega_{21} & \Omega_{22} \end{bmatrix} = \Psi_L \ \Psi_{L-1} \ \ldots \ \Psi_1, \quad \text{Eqn. 9;}$$

with the matrix Ψ_l defined as:

Eqn. 10;

$$\Psi_l = \frac{1}{(1 + \cos\alpha)\left(1 - e^{-\frac{TR}{T1}}e^{j\theta l}\right)} \cdot \begin{bmatrix} 2e^{-\frac{TR}{T2}} \cdot \left(\cos\alpha - e^{-\frac{TR}{T1}}e^{j\theta l}\right) & (1 - \cos\alpha)\left(1 + e^{-\frac{TR}{T1}}e^{j\theta l}\right) \cdot e^{-j\theta l^2} \\ -(1 - \cos\alpha)\left(1 + e^{-\frac{TR}{T1}}e^{j\theta l}\right)e^{j\theta l^2} & 2e^{\frac{TR}{T2}}\left(1 - e^{-\frac{TR}{T1}}\cos\alpha \cdot e^{j\theta l}\right) \end{bmatrix}.$$

where l=1, . . . , L, where L is an integer determined to satisfy the following condition:

$$\frac{\theta}{2} \cdot L = N \cdot \pi \ (N = 0, 1, 2, 3, \ldots). \quad \text{Eqn. 11;}$$

with N is the minimum integer number to satisfy Eqn. 11. For example, if $\theta=2^\circ=\pi/90$, the smallest value of N that satisfies Eqn. 11 is 1, and L=180. Importantly, the present disclosure recognizes that the phase difference, φ, between S^+ and S^- is sensitive to T2.

Now the phase difference can be defined as:

$$\Delta = \arctan\left(\frac{s^t}{s^-}\right). \quad \text{Eqn. 12}$$

To show the dependency of Δ on T1, T2, and FA, Δ with variable parameters was calculated using equations 3, 4, and 12. In particular, FIG. **3** includes a series of plots where the

first plot **300** shows a phase difference with fixed T1 and FA, and variable T2. The phase decreases monotonically with small RF phase increment as T2 increases. As shown in the second plot **302** and third plot **304**, Δ is less sensitive to T1 and FA. The equations and the calculation based on them reveals that T2 can be estimated from the phase difference. More particularly, the first plot **300** shows the phase difference plotted against T2, whereas the second plot shows the phase difference against T1, the third plot shows the phase difference against the FA. The phase was calculated using equations 3, 4, and 12 with small RF phase increments of 1, 2, and 4 degrees. Thus, the present disclosure recognizes and the plots show that the phase difference is sensitive to T2 over a wide range of T2, while the phase is relatively less sensitive to T1 and FA. With this recognition, the present invention provides efficient systems and methods for providing T2 maps using pulse sequences such as the one described above that utilize a phase increment.

With the MR data acquired such as described above, phase correction and reconstruction can be performed. Referring to FIG. **4**, phase errors induced by eddy current of k-space can be corrected using calibration acquisitions consisting of positive and negative readouts. To remove the effect of eddy current, the phase of the acquired k-space is corrected along readout (RO) direction using calibration data. The 0^{th} and 1^{st} order of phase error components are estimated using non-linear optimization method.

In particular, in the three echo-DESS acquisition provided as an example above, RF excitation is performed with a quadratic phase modulation of θ, as described. As described and illustrated, the acquisitions include two FISP echoes (S_1^+ and S_2^+) followed by PSIF echo (S_1^-) with different TEs of TE_1, TE_2, TE_3 and calibration acquisitions can be incorporated into the acquisition. These echoes are modulated with B0− and eddy current-induced phase components. The echoes can be expressed as:

$$S_1^+ = S^+ e^{i(\psi TE_1 + \delta_1)} \quad \text{Eqn. 13;}$$

$$S_2^+ = S^+ e^{i(\psi TE_2 + \delta_2)} \quad \text{Eqn. 14;}$$

$$S_1^- = S^- e^{i(\psi TE_3 + \delta_3)} \quad \text{Eqn. 15;}$$

where ψ is off-resonance, and δ_1-δ_3 are the eddy current-induced phase errors for S_1^+, S_2^+, and S_1^-. Since gradient switching induces the 0^{th} and 1^{st} components of phase errors, δ_1-δ_3 can be expressed as:

$$\delta_1 = a_1 x + b_1 \quad \text{Eqn. 16;}$$

$$\delta_2 = a_2 x + b_2 \quad \text{Eqn. 17;}$$

$$\delta_3 = a_3 x + b_3 \quad \text{Eqn. 18;}$$

where a and b are the constant coefficients, and x is the spatial coordinate along the readout gradient. When the polarity of the gradient is inverted, only the eddy current-induced phase is inverted.

Therefore, referring to FIG. **4**A, the process **400** begins with inputs of the calibration of k-space with positive RO direction **402**, calibration of k-space with negative RO direction **404**, and unconstrained k-space **406**. For each, a 1D fast Fourier transform (FFT) is performed along the RO direction **408**, **410**, **412**. A non-linear optimization is then used at process block **414** to estimate the 0^{th} and 1^{st} order of phase error components. These coefficients can be determined by fitting the phase difference between signals with positive and negative readout gradients. For example, referring to FIG. **4**B, a graph is provided that illustrates that the coefficients in Eqns. 16-18 can be determined by fitting the phase difference between signals with positive and negative readout since only the eddy current-induced phase depends on the polarity of the gradient.

Thus, at process block **416**, the phase errors of δ_1-δ_3 can be corrected by demodulating the phase derived from the Eqns. 16-18 determined by the fitting and, at process block **418**, a 1D FFT is performed.

Referring to FIG. **5**, a reconstruction process **500** in accordance with the present disclosure begins with the phase corrected images for the S_1^+ echo **502**, S_2^+ echo **504**, and the S_1^- echo **506**. That is, after correcting the eddy current-induced phase error, Eqns. 13-15 are simplified as:

$$S_1^+ = S^+ e^{i(\psi TE_1)} \quad \text{Eqn. 19;}$$

$$S_2^+ = S^+ e^{i(\psi TE_2)} \quad \text{Eqn. 13;}$$

$$S_1^- = S^- e^{i(\psi TE_3)} \quad \text{Eqn. 13;}$$

Since echo times are known, off-resonance ψ can be estimated by subtracting the phase between S_1^+ and S_2^+. The S_1^+ echo **502** and the S_2^+ echo **504** are used in a phase subtraction and unwrapping at process block **508**. This can be used to yield a B_0 field map **510** and the B_0-induced phase error can removed by demodulating the phase using the estimated ψ at process block **512** and **514**, which yields a demodulated S_1^+ **516** and demodulated S_1^- **518**. At process block **520** a subtraction is performed that yields a phase difference of S_1^+ and S_1^-, which can be used to reconstruct a T2 map **526** at process block **524**. Alternatively, both the S_1^+ and S_2^+ may be used in the subtraction with S_1^-, which increases SNR. Furthermore, if additional echoes are acquired, those may also be used with S_1^+ and S_2^+. Regardless of the particular signals used, the reconstruction **524** can use a lookup table (LUT) for phase-based T2 estimation. The LUT can be calculated using equations 3-5. If desired, the LUT can use an assumption of T1, for example, an assumption of 1000 ms. The estimation of T2 can be performed by matching the phase difference of S_1^+ (and any additional signals) and S_1^- **522** with the LUT.

EXAMPLE

Phantom and in vivo studies were performed using the systems and methods described above. T2 values of a phantom were measured using the multi-echo spin-echo (MESE) and the systems and methods described above. The phantom consisted of 16 vials and each vial was constructed with a varying concertation of $NiCl_2$ (0 mM, 0.5 mM, 1 mM, 2 mM) and Agar (0.5%, 1%, 2%, 4%) to modulate different T1 and T2. T2 mapping of the brain was also acquired. Healthy volunteers were recruited from an Institutional Review Board (IRB) approved database of healthy volunteers after signing informed written consent. Acquisition parameters are shown in Table 1.

TABLE 1

	Phantom	Brain
(a) Parameters for MESE		
TR	1000 ms	1000 ms
TEs	7/14/22/29/37/ 44/51/59 ms	7/14/22/29/37/ 44/51/59 ms
FOV	20 × 20	20 × 20
Bandwidth	244 Hz/Pix	244 Hz/Pix
Matrix Size	256 × 160	256 × 160
Number of Slices	1	8
Slice Thickness	4 mm	4 mm

TABLE 1-continued

	Phantom	Brain
Scan Time	2:44	2:44
(b) Parameters for the proposed method		
TR	8.0 ms	8.0 ms
TEs	1.4/3.3.6/6.0	1.4/3.3.6/6.0
FOV	20 × 20	20 × 20
Bandwidth	488 Hz/Pix	488 Hz/Pix
Flip Angle	18°	18°
Matrix Size	160 × 160 × 24	160 × 160 × 24
Slice Thickness	4 mm	4 mm
Scan Time	0:33	0:33

T2 maps of the phantom measured using the systems and methods described herein are shown in FIG. **6**A. T2 values agreed well (R^2=0.99) with those measured using MESE, although slight overestimation of the proposed method was observed, as shown in FIG. **6**B. The slopes of the linear regression of the plot, as illustrated in FIG. **6**C, were 1.18 (95% CI=1.12 to 1.24) and −17.1 (95% CI=−11.9 to −22.3).

Referring to FIG. **7**, the T2 maps acquired of the brain using the MESE and proposed method are provided. T2 values of white matter, gray matter, and CSF estimated using the proposed method were 60 (±11), 78 (±9.7), and 401 (±186) ms, while those using MESE were 62 (±2.5), 73 (±2.8), and 354 (±70).

Thus, a new system and method was developed and demonstrated for T2 mapping using an RF phase-modulated acquisition strategy. T2 was estimated from the phase difference of FISP and PSIF signals using the lookup table approach. Phantom and in vivo studies demonstrate the feasibility of the proposed method to enable fast three-dimensional T2 mapping.

The systems and methods described herein can utilize a single acquisition, which enables faster T2 mapping without the potential for misregistration between two separate acquisitions, which is a substantial distinction from previously described T2 mapping methods that require the use of multiple acquisitions. Conventional DESS-based T2 enables T2 mapping with one acquisition. However, it utilizes magnitude information for an estimation, which may be biased by T2*. On the other hand, since the system and methods described herein provide a phase-based method, the results provided using the systems and methods described herein to not depend on T2*.

Thus, a new phase-based T2 mapping system and method are provided that can utilize a multi-echo steady-state pulse sequence. These systems and methods can be modified without deviating from the scope of the systems and methods described herein.

For example, so-called DIXON-based methods can be used for fat-water separation using multiple echoes acquired using the systems and methods described herein. For example, more than three echoes can be used to separate water and fat components and estimate T2 maps of water and fat.

As another example, water excitation can be performed to avoid fat signal. For example, a fat suppression pulse (chem-sat pulse) may affect the steady-state of underlying DESS pulse sequence. Thus, a water only excitation pulse can be used instead of fat suppression methods.

Also, additional external calibration B_0 mapping can be performed to achieve the two echo-DESS sequence. In this case a S_2^+ echo is not required anymore, which results in shorter TR and reduced scan time.

Furthermore, simultaneous T1/T2 mapping can be performed by using multiple flip angles. In particular, multiple acquisitions can be performed with different flip angles to encode T1 information into the magnitude of the signal and use the above-described phase-based method to generate the T2 map.

Further still, diffusion information can be encoded in the acquired data by increasing gradient moment. A spoiling gradient can be used to induce diffusion, which results in both phase shifts and magnitude attenuation, the combination of which can be used to encode the apparent diffusion coefficient of the underlying tissue.

Finally, simultaneous T1/T2-weighted imaging can be performed. For example, the present disclosure recognizes the dependence of the signal phase and magnitude on T2 of the tissue, at low RF phase increments ($\Delta\phi$). For low $\Delta\phi$ (on the order of just a few degrees), there is a strong dependence of the measured phase on the T2 of the tissue. That is, the magnitude of the signal (η) shows moderate dependence on T2, weak dependence on flip angle for flip angles larger than 10°, and heavy dependence on T1. However, there are some special cases of particular larger increments greater than, for example, 1-5° that preserve the transverse magnetization, for example, 32.2°. Regardless of the particular value of the increment, the present disclosure recognizes that, when the increment is properly selected, the phase differences are elicited that can be advantageously utilized. The present disclosure can use phase increments to induce distinct results in amplitude versus phase and create systems and methods to improved clinical results by creating a pulse sequence where both T1w and T2w data can be acquired during the same GRE or SGRE pulse sequence, thereby, eliminating the need for multiple acquisitions, such as multiple FSE acquisitions or combinations of FSE and SGRE acquisitions, such as described in co-pending U.S. patent application Ser. No. 17/184,768, which is incorporated herein by reference in its entirety.

The systems and methods described herein find substantial and diverse clinical applications, including brain imaging, cardiac imaging (including transplant rejection), liver imaging (including to study inflammation and fibrosis in diffuse liver disease, and also liver iron overload), cartilage imaging, and applications where pathology is known to alter the T2 and T1 of the underlying tissue.

The present invention has been described in terms of one or more preferred embodiments, and it should be appreciated that many equivalents, alternatives, variations, and modifications, aside from those expressly stated, are possible and within the scope of the invention.

The invention claimed is:

1. A magnetic resonance imaging (MRI) system comprising:

a magnet system configured to generate a static magnetic field (B_0) about at least a portion of a subject arranged in the MRI system;

a plurality of gradient coils configured to apply magnetic gradients to the polarizing magnetic field;

a radio frequency (RF) system configured to apply an excitation field to the subject and acquire MR image data from the subject;

a computer system programmed to:

control the plurality of gradient coils and the RF system to perform a gradient echo pulse sequence that includes a phase increment of an RF pulse of the gradient echo pulse sequence selected to induce a phase difference between two echoes selected to be similar, other than echo time (TE);

control the RF system to acquire MR data corresponding to at least the two echoes selected to be similar, other than TE;

derive a B_0 map using the MR data corresponding to the two echoes selected to be similar, other than TE; and

use the B_0 map and MR data from at least one of the two echoes selected to be similar, other than TE, generate a map of T2 of the subject.

2. The MRI system of claim **1**, wherein the computer is further programmed to control the plurality of gradient coils and the RF system to acquire MR data corresponding to a third echo at a third TE and wherein, to derive the B_0 map the computer system uses the MR data corresponding to a first of the two echoes selected to be similar, other than TE and the MR data corresponding to the third echo.

3. The MRI system of claim **2**, wherein the MR data corresponding to the first of the two echoes is a fast imaging with steady-state precession (FISP) echo (S_1^+) and the third echo is a time reversed fast imaging with steady state precession (PSIF) echo (S_1^-).

4. The MRI system of claim **3**, wherein the B_0 map is used to demodulate B_0 phase components of the S_1^+ echo and the S_1^- echo to generate the map of T2.

5. The MRI system of claim **4**, wherein the computer system is further configured to subtract demodulated MR data corresponding to the S_1^+ echo and the S_1^- echo and compare a result of the subtraction to a look up table to generate the map of T2.

6. The MRI system of claim **3**, wherein the second of the two echoes is a fast imaging with steady-state precession (FISP) echo (S_2^+).

7. The MRI system of claim **1**, wherein the phase increment is formed using a quadratic increase of transmitting phase to encode T2 information into the phase of the at least two echoes.

8. The MRI system of claim **1**, wherein the computer system is further configured to control the plurality of gradient coils to apply positive readout gradients and negative gradients as calibration acquisitions without phase-encoding to remove eddy current-induced phase error.

9. The MRI system of claim **8**, wherein the computer system is further configured to perform the calibration acquisitions using two additional phase encoding lines coupled with a slab encoding gradient.

10. The MRI system of claim **1**, wherein the computer system is further configured to control the RF system to acquire MR data corresponding to more than the at least the two echoes and perform a fat and water separation method.

11. A method for producing at least one of an image or a map of a subject comprising:

controlling a magnetic resonance imaging (MRI) system to perform a pulse sequence that includes a phase increment of an RF pulse selected to induce a phase difference between two echoes at different echo times (TE);

controlling the MRI system to acquire MR data corresponding to at least the two echoes at different TEs;

deriving a static magnetic field (B_0) map of the MRI system using the MR data corresponding to the two echoes; and

using the B_0 map and MR data from at least one of the two echoes, generate a map of T2 of the subject.

12. The method of claim **11**, further comprising acquiring MR data corresponding to a third echo at a third TE and wherein, deriving the B_0 map includes using the MR data corresponding to a first of the two echoes and the MR data corresponding to the third echo.

13. The method of claim **12**, wherein the first echo is a fast imaging with steady-state precession (FISP) echo (S_1^+) and the third echo is a time reversed fast imaging with steady state precession (PSIF) echo (S_1^-).

14. The method of claim **13**, further comprising demodulating B_0 phase components of the S_1^+ echo and the S_1^- echo using the B_0 map to generate the map of T2.

15. The method of claim **14**, further comprising subtracting demodulated MR data corresponding to the S_1^+ echo and the S_1^- echo and comparing a result of subtracting demodulated MR data to a look up table to generate the map of T2.

16. The method of claim **13**, wherein the second of the two echoes is a fast imaging with steady-state precession (FISP) echo (S_2^+).

17. The method of claim **11**, wherein the phase increment is formed using a quadratic increase of transmitting phase to encode T2 information into the phase of the at least two echoes.

18. The method of claim **11**, further comprising applying positive readout gradients and negative gradients as calibration acquisitions without phase-encoding to remove eddy current-induced phase errors.

19. The method of claim **18**, further comprising performing the calibration acquisitions using two additional phase encoding lines coupled with a slab encoding gradient.

20. The method of claim **11**, further comprising acquiring MR data corresponding to more than the at least the two echoes and performing a fat and water separation method.

* * * * *